Image reconstruction using the phase variance algorithm

J.R. Fienup

Optical Science Laboratory
Advanced Concepts Division
Environmental Research Institute of Michigan
P.O. Box 8618, Ann Arbor, MI 48107

ABSTRACT

In many imaging situations the quality of the image is degraded by phase errors. In this paper we describe an algorithm for correcting phase errors. It is applicable to cases in which the phase-error-degraded complex Fourier transform of the aberrated image is available; these include imaging with heterodyne sensors or with interferometric sensors. The phase-error correction algorithm is a variation on the iterative Fourier transform (phase retrieval) algorithm. It uses a support constraint on the object, making it useful for imaging bright objects on dark backgrounds. It can be extended to include uncertainties in both the modulus and the phase of the Fourier transform.

1. INTRODUCTION

1.1 Background

We wish to form an image of an object, f(x, y), which may be complex-valued or real and non-negative, from measurements of its Fourier transform,

$$F(u, v) = |F(u, v)| \exp[i\psi(u, v)] = \iint f(x, y) \exp[-i2\pi(ux + vy)]\, dxdy \quad . \tag{1}$$

For the phase retrieval problem we have only the Fourier modulus, |F(u, v)|, and wish to retrieve the Fourier phase, $\psi(u, v)$, or equivalently reconstruct the object. This can usually be accomplished using the iterative Fourier transform algorithm if the object is real-valued and non-negative,[1,2] assuming a bright object on a dark background. On the other hand, phase retrieval is very difficult for complex-valued objects, unless the object is a special type,[3] such as having separated parts or glints.

In some situations one has the ability to make additional measurements that makes phase retrieval easier for complex-valued objects.

1.2 Imaging with partial phase information

One kind of such additional information is partial phase information. Partial phase information can come from an imaging system that inherently measures or determines the phase. Two major cases of partial phase information are: (1) phase known well over a small aperture and (2) noisy phase over the entire aperture. In the first case it is a matter of filling in the missing phase, but most of the phase is missing. This is discussed in Reference 4. In the second case it is a matter of correcting the errors in the given phase. The latter is the subject of this paper. Many different imaging systems could provide data for this second case, that of noisy phase known over the entire aperture. They include active imaging modalities such as heterodyne array measurements or synthetic aperture radar and passive modalities such as astronomical speckle interferometry using triple correlation and aperture-plane interferometry using phase closure.

The basic approach to phase retrieval and image reconstruction for these scenarios is to use the iterative Fourier transform algorithm to take advantage of all the available data and constraints to form the solution. This approach allows for the combination of a variety of disparate types of information, such as Fourier modulus (square root of intensity), Fourier phase, object-domain support (finite extent) constraint, and nonnegativity (applicable for incoherent images).

If the partial phase information is nearly complete, so that using that phase yields a useful image, then the phase-retrieval algorithm can be thought of as a way to clean up the image to improve its quality. This is equivalent to reducing the errors or filling in the gaps in the given partial phase information. If the partial phase information is very incomplete or noisy, then no useful image would result from it, and the phase-retrieval algorithm would be forming the image in the first place, with the partial phase information helping it to succeed.

1.3 The iterative transform algorithm

One iteration of the iterative transform algorithm, for solving the phase retrieval problems, consists of the following four steps (for the k^{th} iteration):

(1) Fourier transform an input image, $g_k(x, y)$, yielding $G_k(u, v) = |G_k(u, v)| \exp[i\phi_k(u, v)]$.

(2) Force G_k to satisfy the measured Fourier modulus:
$G_k'(u, v) = |F(u, v)| \exp[i\phi_k(u, v)]$.

(3) Inverse Fourier transform $G_k'(u, v)$ to yield the image $g_k'(x, y)$.

(4) Choose a new input image, $g_{k+1}(x, y)$, based on how $g_k'(x, y)$ violates the object-domain constraint(s).

The fourth step is best performed using the hybrid input-output (HIO) version of the iterative transform algorithm:

$$g_{k+1}(x, y) = \begin{cases} g_k'(x, y), & (x, y) \notin \gamma \\ g_k(x, y) - \beta\, g_k'(x, y), & (x, y) \in \gamma \end{cases} , \qquad (2)$$

where γ is the set of points for which $g_k'(x, y)$ violates the object-domain constraints and β is a feedback constant ($\beta = 0.7$ usually works well). The error-reduction (ER) version of the algorithm, for which

$$g_{k+1}(x, y) = \begin{cases} g'_k(x, y) & , \quad (x, y) \notin \gamma \\ 0 & , \quad (x, y) \in \gamma \end{cases} , \tag{3}$$

is typically less useful because it converges to a solution extremely slowly.[5]

2. THE PHASE VARIANCE ALGORITHM

In what follows is described a modification of the iterative transform algorithm which uses a poorly-known phase across the Fourier-domain aperture.

Let the object and its Fourier transform be f(x, y) and $F(u, v) = |F(u, v)| \exp[i\Psi(u, v)]$, respectively. Suppose we measure

$$G_o(u,v) = |G_o(u,v)| \exp[i\theta(u,v)]$$

$$= F(u,v) \exp[i\phi_e(u,v)] = |F(u,v)| \exp\{i[\Psi(u,v) + \phi_e(u,v)]\} \tag{4}$$

where $\phi_e(u, v)$ is a phase error with known (or approximately known) variance σ^2. So the measured (noisy) phase is

$$\theta(u,v) = [\Psi(u,v) + \phi_e(u,v)]_{\text{mod}2\pi} \quad . \tag{5}$$

The blurred image gotten by inverse Fourier transforming $G_o(u, v)$ would be $g_o(x, y)$.

We improve the phase estimate, over that given by the measurement $\theta(u, v)$, using the iterative Fourier transform phase retrieval algorithm which uses additional information in the object domain, such as nonnegativity and/or support constraints to infer the true phase of F(u, v). Two approaches are described below.

The first approach is to perform the usual phase retrieval algorithm, typically cycles of hybrid input-output (HIO) and error-reduction (ER), and simply use $\theta(u, v)$ as the initial estimate for the Fourier-domain phase. The Fourier-domain constraint would be the measured modulus $|G_o(u, v)| = |F(u, v)|$.

The second approach is to constrain the phase during the iterations to lie near $\theta(u, v)$. Constraining the phase to equal $\theta(u, v)$ does no good since one would simply get the blurred image with no change. Instead it is more useful to allow the phase to wander from $\theta(u, v)$, but not allow it to wander too far. This can be accomplished using the phase variance algorithm, which is described as follows. In the Fourier domain, as well as constraining the modulus to equal $|F(u, v)|$, constrain the phase to not differ from $\theta(u, v)$ by more than $c\sigma$, where c, the variance factor, is a real constant on the order of unity. In order to account for 2π ambiguities, this should be performed as follows, where ϕ is the phase of the Fourier transform of the input object to the iterative loop and ϕ' is the altered phase:

$$\phi' = \begin{cases} \theta - c\sigma & , \quad (\phi - \theta)_{\mathrm{mod}2\pi} < -c\sigma \\ \phi & , \quad -c\sigma \le (\phi - \theta)_{\mathrm{mod}2\pi} \le c\sigma \\ \theta + c\sigma & , \quad (\phi - \theta)_{\mathrm{mod}2\pi} > c\sigma \end{cases} \quad . \tag{6}$$

This Fourier operation is illustrated in Figure 1. Figure 2 shows a block diagram of the iterative Fourier transform algorithm including the partial phase information, $\theta(u, v)$.

Several variations of the phase variance algorithm were attempted for both the cases of a real, non-negative object and a complex-valued object. In the object domain one can use either the hybrid input-output (HIO) or error-reduction (ER) algorithm while one employs the phase variance algorithm in the Fourier domain. We refer to these two combinations as PVHIO and PVER, respectively. Although HIO usually performs better than ER, we found that PVER usually performs better than PVHIO. Generally c in the range of 0.6 to 1.0 worked the best.

After about twenty iterations of PVER the algorithm tends to stagnate. At this point, in order to achieve further improvement, we continue with the traditional iterative transform algorithm, using cycles of HIO and ER, no longer constraining the Fourier phase. A good approach is to perform twenty iterations of PVER with $c = 0.8$, then ten iterations of ER, and finally several cycles, each cycle consisting of 20 HIO ($\beta = 0.7$) and 10 ER, until stagnation (no further progress) occurs. After every other cycle, we enlarge the support constraint by adding to it each nearest-neighbor pixel that was previously outside the support. In order to reduce sidelobes in the image, to make the support constraint more effective when diffraction effects are included, the Fourier modulus should be weighted with an apodizing function. For the experiments described in what follows, we used a weighting function proportional to the autocorrelation of a circle.

The progress of the iterative transform algorithm is monitored by computing the object domain error metric,

$$\mathrm{ODEM} = \sqrt{\frac{\sum_{x \epsilon \gamma} |g'(x, y)|^2}{\sum_{x} |f(x, y)|^2}} \quad , \tag{7}$$

where γ is the set of points at which $g'(x, y)$ violates the object-domain constraints. For these digital simulation experiments, in which we also know the actual object, we can also compute the absolute error,

$$\mathrm{ABSERR} = \sqrt{\frac{\sum_{x} |\alpha g'(x - x_s, y - y_s) - f(x, y)|^2}{\sum_{x} |f(x, y)|^2}} \quad , \tag{8}$$

where (x_s, y_s) is the shift of the output image $g'(x, y)$, and α is the scale factor, that maximizes its correlation with the true object $f(x, y)$. For images that are recognizable and have some utility, ABSERR is typically below 0.5. For images that are good representations of the object, ABSERR is typically about 0.3 or less.

3. EXPERIMENTAL RESULTS

3.1 Real, nonnegative objects

Phase retrieval using the iterative transform algorithm is usually successful for the case of real, nonnegative objects. With noisy phase data and using the phase variance algorithm, we found that convergence to the solution was more reliable (less likely to stagnate) and required fewer iterations.

3.2 Complex-valued objects

The reconstruction of complex-valued objects is much more difficult since one no longer has the powerful nonnegativity constraint. For the complex-valued, speckled object shown in Figure 3(A) the conventional iterative transform algorithm, when started with a random initial estimate, yielded the unrecognizable image shown in Figure 3(C). When the noisy phase was used to start the algorithm, however, the conventional iterative transform algorithm improved the image quality substantially, although the reconstructed image remained imperfect. The phase variance algorithm similarly reconstructed a substantially improved, but imperfect image. The results from the phase variance algorithm were slightly better than those of the conventional algorithm for these cases. The initial support constraint shown in Fig. 3(B) was obtained from the Fourier modulus using the triple intersection approach.[6] Phase errors used for these experiments were generated using McGlammery's method.[7] These phase errors are similar to those that would result from atmospheric turbulence. The adjustable parameters of the phase errors are the standard deviation, σ, and the correlation length, corl. The improvement in quality of the reconstructed images, shown in the bottom row of Figure 3, over that of the given blurred images, shown in the middle row, is substantial.

Image reconstruction experiments were performed for the case of Fourier modulus data corrupted by photon noise. The iterations improved the RMS error of the image for the cases of more than 120 photons per aperture-plane speckle (or 10^5 total photons). However, for lower light levels, the algorithm can make the image worse. This happens when the Fourier modulus data is noisier than the phase data; then adjusting the phase to be more consistent with the noisy modulus data is counterproductive. In such a case it would actually make sense to adjust the modulus to be more consistent with the phase data. Figure 4 shows the RMS error of the reconstructed image as a function of the total number of photons. Figure 5 shows three of the blurred images and the corresponding improved images reconstructed from noisy data using the phase variance algorithm.

4. SUMMARY AND CONCLUSIONS

In summary, we have developed a new variation, the phase variance algorithm, of the iterative transform algorithm which reconstructs a fine resolution image from Fourier modulus measurements when degraded Fourier phase data is available. For real, nonnegative objects it converges faster and more reliably than the conventional iterative transform algorithm using no phase information. For complex-valued objects, which are difficult to reconstruct, it reconstructs images of quality substantially better than that of the blurred images given by the available noisy phase data.

Other variations of the phase variance algorithm are possible which may yield improved performance. Rather than using a formula for the new phase estimate such as Eq. (6) which abruptly changes at a threshold value, it may be better to have a formula that changes continuously and smoothly with the data. An example of such a formula would be

$$\phi' = \theta + c\sigma \ln[1 + |\phi - \theta|/(c\sigma)] \operatorname{sign}(\phi - \theta) \quad , \tag{9}$$

which is approximately equal to ϕ for $|\phi - \theta| << c\sigma$ and departs slowly from the neighborhood of θ when $|\phi - \theta| >> c\sigma$.

Another interesting possibility is to use the same type of operation on the modulus of the Fourier transform. That is, rather than substitute the measured Fourier modulus for the computed Fourier modulus, allow the Fourier modulus wander from the measured value according to the amount of noise present in the Fourier modulus data. Such an algorithm would reconstruct the phase from the modulus or the modulus from the phase depending on which has the higher signal-to- noise ratio at any given point in the Fourier domain.

5. ACKNOWLEDGEMENT

This research was funded by the Air Force Weapons Laboratory through the Wright Research and Development Center.

6. REFERENCES

1. J.R. Fienup, "Reconstruction of an Object from the Modulus of Its Fourier Transform," Opt. Lett. 3, pp. 27-29, 1978.

2. J.R. Fienup and C.C. Wackerman, "Phase Retrieval Stagnation Problems and Solutions," J. Opt. Soc. Am. A 3, pp. 1897-1907, 1986.

3. J.R. Fienup, "Reconstruction of a Complex-Valued Object from the Modulus of Its Fourier Transform Using a Support Constraint," J. Opt. Soc. Am. A 4, pp. 118-123, 1987.

4. J.R. Fienup and A.M. Kowalczyk, "Phase retrieval for a Complex-Valued Object by Using a Low-Resolution Image," J. Opt. Soc. Am. A 7, pp. 450-458, 1990.

5. J.R. Fienup, "Phase Retrieval Algorithms: A Comparison," Appl. Opt. 21, pp. 2758-2769, 1982.

6. T.R. Crimmins, J.R. Fienup, and B.J. Thelen, "Improved Object Support from Autocorrelation Support and Application to Phase Retrieval," J. Opt. Soc. Am. A 7, 3-13, 1990.

7. B.L. McGlammery, "Computer Simulation Studies of Compensation of Turbulence Degraded Images," in J.C. Urbach, ed., Image Processing, Proc. SPIE 74, pp. 225-233, 1976.

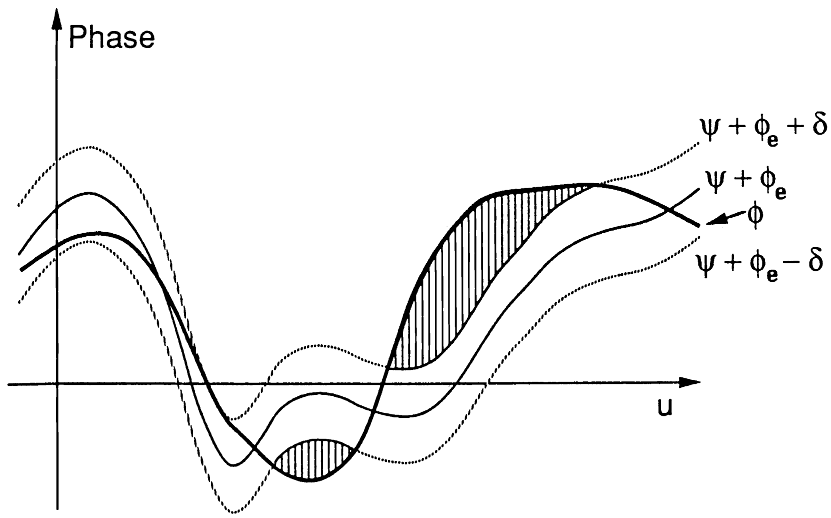

Figure 1. Fourier-domain phase modification by the phase variance algorithm. The phase $\phi'(u,v)$ is constrained to lie within $\delta = c\sigma$ of the given phase, $\theta(u,v) = \psi(u,v) + \phi_e(u,v)$.

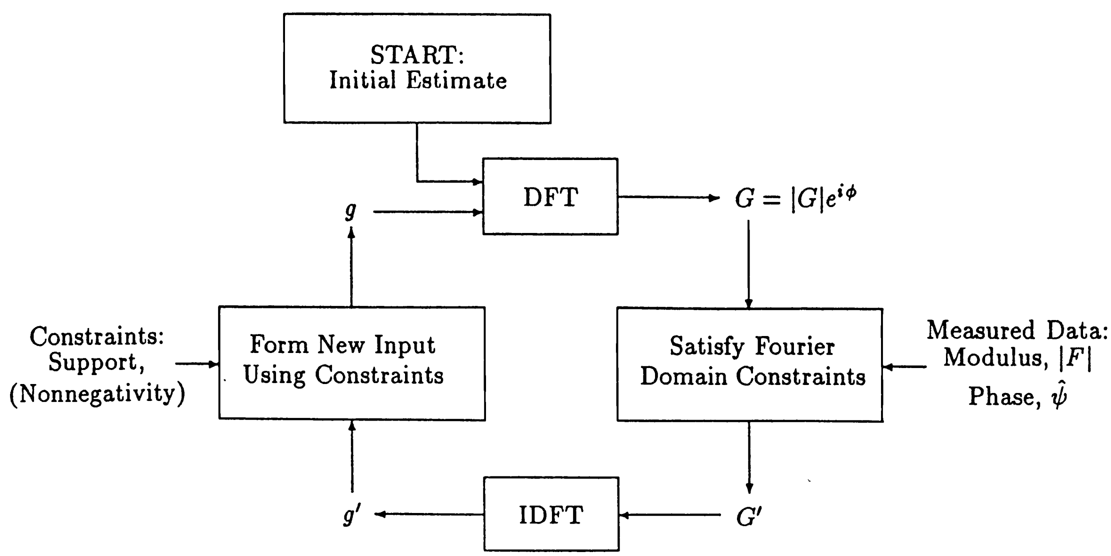

Figure 2. Block diagram of the phase variance version of the iterative transform algorithm.

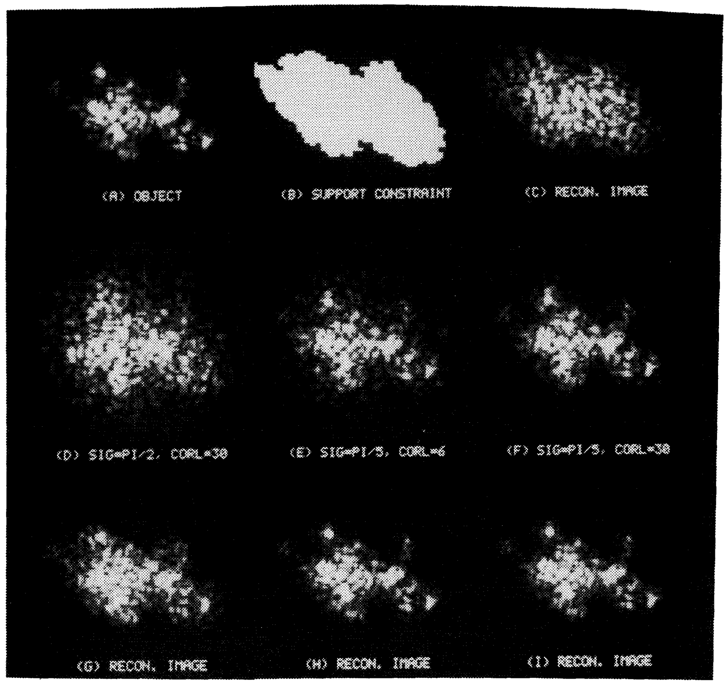

Figure 3. Reconstruction of complex-valued images by the phase variance algorithm. (a) Object; (b) support constraint; (c) image reconstructed with no phase information; (d)-(f) blurred images, with (d) phase errors $\sigma = \pi/2$ radians and corl = 30 pixels, with (e) $\sigma = \pi/5$ and corl = 6, and with (f) $\sigma = \pi/5$ and corl = 30; and (g) - (i) corresponding images reconstructed by the phase variance algorithm.

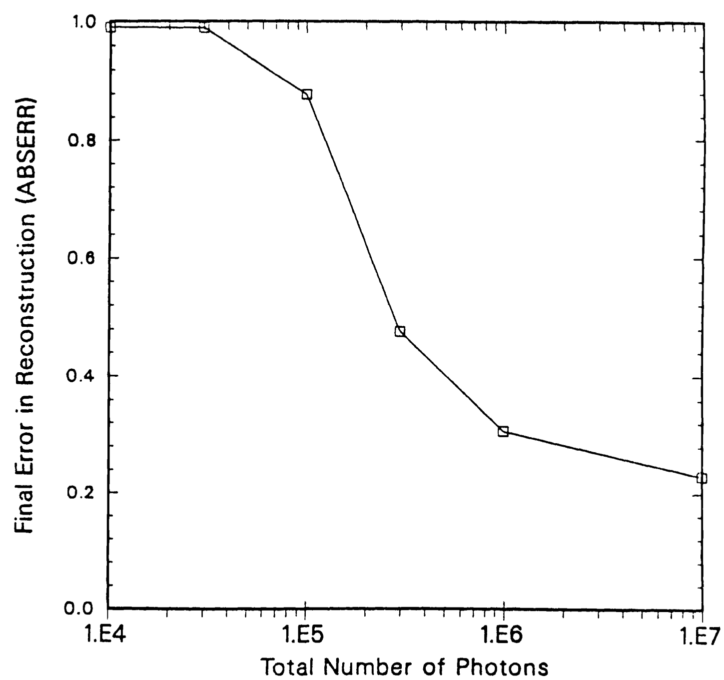

Figure 4. RMS error of the reconstructed images as a function of the total number photons.

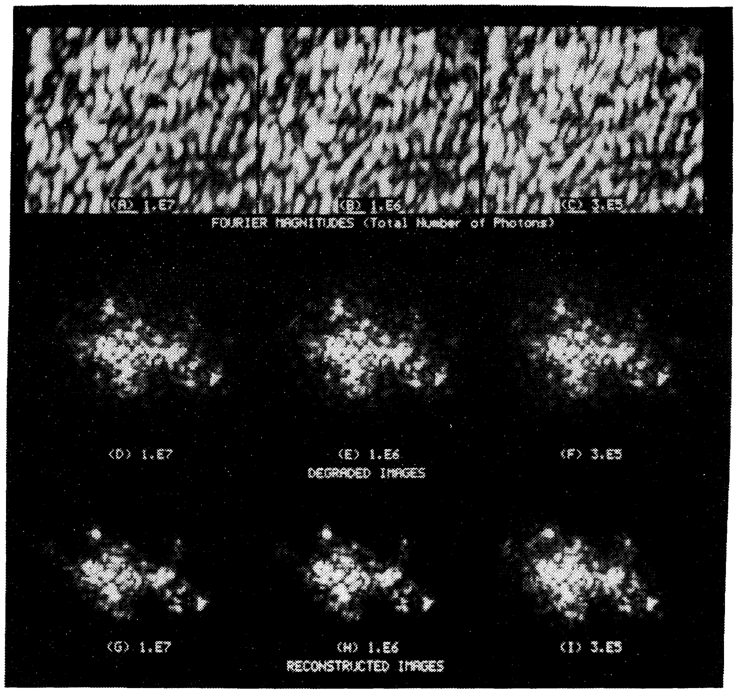

Figure 5. Reconstruction of complex-valued images by the phase variance algorithm with photon noise. (a) - (c) Noisy Fourier modulus estimates (their squares, the intensities, were subjected to photon noise), with (a) 10^7, (b) 10^6, and (c) 3×10^5 total photons; (d) - (f) images degraded by the phase error; and (g) - (i) the corresponding reconstructed images.